Quantitation of Myocardial Fatty Acid Metabolism Using PET

Steven R. Bergmann, Carla J. Weinheimer, Joanne Markham and Pilar Herrero

Cardiovascular Division, Washington University School of Medicine, St. Louis, Missouri

Abnormalities of fatty acid metabolism in the heart presage contractile dysfunction and arrhythmias. This study was performed to determine whether myocardial fatty acid metabolism could be quantified noninvasively using PET and 1-^{11}C-palmitate. **Methods:** Anesthetized dogs were studied during control conditions; during administration of dobutamine; after oxfenicine; and during infusion of glucose. Dynamic PET data after administration of 1-^{11}C-palmitate were fitted to a four-compartment mathematical model. **Results:** Modeled rates of palmitate utilization correlated closely with directly measured myocardial palmitate and total long-chain fatty acid utilization (r = 0.93 and 0.96, respectively, p < 0.001 for each) over a wide range of arterial fatty acid levels and altered patterns of myocardial substrate use (fatty acid extraction fraction ranging from 1% to 56%, glucose extraction fraction from 1% to 16% and myocardial fatty acid utilization from 1 to 484 nmole/g/min). The percent of fatty acid undergoing oxidation could also be measured. **Conclusion:** The results demonstrate the ability to quantify myocardial fatty acid utilization with PET. The approach is readily applicable for the determination of fatty acid metabolism noninvasively in patients.

Key Words: palmitate; mathematical models; oxidation; tracers

Under physiological circumstances, 60% to 80% of myocardial energy use is supplied by oxidation of long-chain fatty acids (*1–4*). This declines after a carbohydrate meal because of the inhibitory influence of insulin on peripheral lipolysis and the dependence of myocardial fatty acid use on the arterial concentrations.

Derangements in myocardial fatty acid metabolism are multiple. They can be inherited (*5*) or acquired (*1–4*). Impairment of beta-oxidation of fatty acids is a hallmark of myocardial ischemia.The decline in contractile function, as well as the onset of arrhythmias, may reflect accumulation of up-stream long-chain fatty acid intermediates (*1–4,6–8*). Viruses, as well as aspirin, have also been shown to impair fatty acid metabolism (*9,10*) and may play a role in some forms of acquired heart failure. Accordingly, noninvasive delineation of fatty acid metabolism with PET has been a long-standing goal (*11*).

Early studies demonstrated that, under certain circumstances, washout of extracted 1-^{11}C-palmitate from the myocardium correlated with myocardial oxygen consumption (*12–15*). Labeled palmitate was useful in delineating zones of myocardial infarction (*11,16,17*) and in characterizing the efficacy of reperfusion strategies (*18–20*). Although the rapid washout of tracer from the myocardium correlated to some extent with the production of $^{11}CO_2$ (indicative of oxidation) and the slower washout correlated with incorporation of tracer into triglycerides (*13–15*), simple exponential analysis was shown to be sensitive to levels of tissue oxygenation as well as to levels of arterial fatty acid and the pattern of substrate use (*21–24*).

Our interest in noninvasive delineation of fatty acid metabolism was rekindled based on the identification of inherited abnormalities in fatty acid oxidation which can lead to cardiomyopathy (*25*) and because it appears that some patients with acquired, nonischemic cardiomyopathy also have abnormalities of fatty acid metabolism (*11,26,27*). The purpose of this study was to validate a compartmental model developed to quantitatively characterize myocardial fatty acid metabolism noninvasively with PET.

MATERIALS AND METHODS

The protocol was approved by the Animal Studies Committee of the Washington University School of Medicine and conformed to the guidelines of the American Heart Association and the American Physiological Society.

General Protocol

Adult, conditioned dogs of either gender weighing 22–28 kg were fasted overnight, sedated with morphine sulfate (2 mg/kg subcutaneously) and anesthetized with thiopental (12.5 mg/kg intravenously), α-chloralose (72 mg/kg intravenously) and a constant infusion of fentanyl (0.3 μg/kg/min). Dogs were intubated and ventilated with room air to maintain arterial pH and blood gases within the physiologic range. Additional chloralose was administered periodically to maintain a stable level of anesthesia.

Catheters were placed in the thoracic aorta via a femoral artery for aortic blood pressure recording, arterial blood sampling and arterial microsphere withdrawal. A femoral vein was catheterized for administration of drugs. A catheter was advanced into the coronary sinus under fluoroscopic guidance from the right internal jugular vein and placed at least 2 cm into the coronary sinus from the right atrium (confirmed with a small amount of contrast). The left atrium was catheterized retrogradely from a femoral artery with a left atrial catheter and used for administration of radiolabeled microspheres. After catheterization, dogs were heparinized with 5000 U intravenously which was repeated every 90 min.

To study a wide range of rates of myocardial fatty acid utilization and patterns of myocardial substrate use, four groups of dogs were studied. Dogs in the control group (n = 6) were studied with no further intervention. To increase myocardial work and concurrently raise arterial fatty acid levels, 5 dogs were given a constant infusion of 5 to 10 μg/kg/min dobutamine. To selectively block fatty acid oxidation, 9 dogs (including 3 studied under control conditions) were given oxfenicine (33 mg/kg intravenously), a potent inhibitor of carnitine palmitoyltransferase I, an enzyme critical for transporting long-chain fatty acids from the cytosol into the mitochondria (*28–30*). The final group of 3 dogs was given an infusion of glucose, insulin and potassium (500 g glucose, 50 U insulin and 70 mg KCl/liter administered at 0.075 ml/kg/min) to increase arterial glucose levels, which diminishes arterial fatty acid levels and thus myocardial fatty acid use. Myocardial glucose utilization increases.

After 30 min of stabilization after each intervention and immediately before the PET emission scan, myocardial blood flow was measured using radiolabeled microspheres. One hundred μCi

TABLE 1
Summary of Hemodynamics, Myocardial Blood Flow and MVO_2

Group (n)	HR	SBP	DBP	RPP	MBF	MVO_2
Control (6)	85 ± 16	122 ± 18	78 ± 14	7607 ± 1869	0.74 ± 0.21	8.03 ± 1.71
Dobutamine (5)	101 ± 36	135 ± 33	79 ± 23	9172 ± 3175	0.84 ± 0.22	11.17 ± 3.44
Oxfenicine (9)	77 ± 25	114 ± 27	69 ± 15	6115 ± 1838	0.54 ± 0.21	5.97 ± 2.43
Glucose (3)	59 ± 9	121 ± 1	62 ± 11	4873 ± 1109	0.55 ± 0.04	6.09 ± 1.20

HR = heart rate (bpm); SBP and DBP = systolic and diastolic blood pressure (mmHg); RPP = rate pressure product (mean arterial pressure × HR, mmHg × bpm); MBF = myocardial blood flow (ml/g/min); and MVO_2 = myocardial oxygen consumption (μmole oxygen/g/min). Results are presented as mean ± s.d.

(2–3 × 10^6, 15 μm spheres) of either strontium-85, cerium-141 or scandium-86 were administered 2 min before each administration of 1-^{11}C-palmitate through the left atrial catheter while blood was being withdrawn from the aortic catheter at 10 ml/min. After completion of the PET study, animals were euthanized with an overdose of anesthesia and the myocardium sectioned into approximately thirty 0.5–0.8-g pieces for quantification of myocardial blood flow by the standard reference technique.

Imaging Protocol

Dogs were studied in a PET VI. Attenuation correction scanning was performed. To identify vascular structures, 20–40 mCi of $C^{15}O$ (which binds to erythrocytes) were administered by inhalation. After waiting 30–60 sec to allow gas clearance from the lungs, a 5-min scan was obtained. After allowing for decay of radioactivity ($t_{1/2}$ of ^{15}O = 2 min), 20–40 mCi of 1-^{11}C-palmitate [prepared as previously described in detail (31)] were administered intravenously as a bolus. Beginning with the time of administration, paired 3-ml arterial and coronary sinus samples were obtained every 30 sec for 3 min, every 1 min for 5 min, every 2.5 min for 15 min and every 5 min to the end of the scanning procedure. Dynamic PET scans were obtained for 30 min consisting of eighteen 5-sec frames, ten 30-sec frames and then 60-sec frames for the remainder of the imaging period. Data were corrected for isotope physical decay.

Analysis of PET Data

Regions of interest (3–5 cm^3) on each slice representing anterior and lateral myocardium as well as a small region within the left atrial blood pool (1 cm^3) (to determine the arterial input function) were interactively placed. Regions near the liver were avoided to obviate spillover of radioactivity from liver to heart. Arterial time-activity curve data corrected for $^{11}CO_2$ (see below) and myocardial time-activity data were analyzed using a four-compartment model (Fig. 1 and Appendix). Tracer entering the mitochondrial compartment was considered to be unidirectional, and washout of $^{11}CO_2$ from the mitochondria to the vasculature was assumed to be proportional to flow. Turnover rate constants, to and from each compartment, blood to myocardial spillover (F_{BM}) and myocardial recovery coefficient (F_{MM}) were estimated by solving simultaneous differential equations. Palmitate utilization, back-diffusion, oxidation and esterification were computed (see Appendix) using a modification of the model described by De Grado et al. (32).

Assessment of Substrate Utilization

At the beginning and end of the PET scan, paired arterial and coronary sinus samples were obtained for assay of fatty acids, glucose and lactate. Steady-state myocardial fatty acid, glucose, lactate and oxygen utilization were calculated from arterial-coronary sinus differences of each substance multiplied by myocardial blood flow. Blood was drawn into vacutainers, placed immediately

on ice, centrifuged within 60 min at 4°C and plasma separated and frozen at −70°C until assay.

Total long-chain fatty acid content was measured using a previously described assay (33). Individual fatty acids were measured by gas chromatography. 0.05 ml of the internal standard, heptadecanoic acid (1.0 mg/ml) and 0.1 ml of 6 N HCl were added to 0.25 to 0.5 ml of plasma. The volume was adjusted to 1.0 ml with distilled water and the mixture vortexed and allowed to sit for 5 min at room temperature. One milliliter of diethyl ether was added and the mixture was vortexed vigorously for 30 sec and then centrifuged for 10 min. The ether layer was removed and the extraction was repeated two more times. The ether layers were combined, evaporated under nitrogen and the residue dissolved in 0.05 ml of iso-octane. Two microliters of this solution were injected onto a gas chromatograph fitted with a Nukol fused silica capillary column (30 m, i.d. 0.53 mm) and eluted isocratically at 190°C. Individual fatty acids (identified using authentic standards) were compared to the internal standard.

Glucose and lactate were assayed enzymatically using a STAT-PLUS glucose/lactate analyzer (Yellow Springs Instrument, Yellow Springs, OH). Paired samples of arterial and coronary sinus blood were also obtained for hematocrit, blood pH, pCO_2, pO_2 and oximetry. To correct the arterial input function for tracer metabolized to $^{11}CO_2$ and to measure conversion of 1-^{11}C-palmitate to $^{11}CO_2$, timed arterial and coronary sinus samples were collected into base as described previously (21). Total ^{11}C-radioactivity was measured in alkalinized blood and non-$^{11}CO_2$ radioactivity (i.e., palmitate) was measured after blood was acidified with 6 N HCl and bubbled with N_2 for 10 min to release $^{11}CO_2$. The $^{11}CO_2$ in each sample was calculated from the difference. Myocardial production of $^{11}CO_2$ was calculated from the $^{11}CO_2$ content of coronary sinus blood corrected for $^{11}CO_2$ in arterial blood. Direct
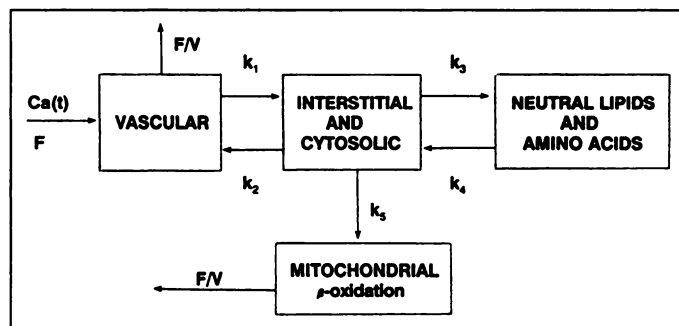

FIGURE 1. Schematic diagram of the four-compartment model. Compartment 1 represents the vascular space; 2, the interstitial and intracellular spaces; 3, neutral lipids, amino acids and other slow turnover pools (even though these occur at different loci physiologically); and 4, mitochondrial beta-oxidation. k_n represents the turnover rate constant between compartments, F = myocardial blood flow, V = vascular volume and Ca(t) = arterial concentration of tracer over time.

TABLE 2
Summary of Substrate Arterial Concentrations, Myocardial Extraction and Utilization

Group (n)	Arterial concentration			Myocardial extraction fraction			Myocardial utilization		
	FA	Glucose	Lactate	FA	Glucose	Lactate	FA	Glucose	Lactate
Control (6)	367 ± 117	5.72 ± 0.95	1.37 ± 0.41	41 ± 9	2 ± 6	40 ± 15	107 ± 42	85 ± 263	413 ± 214
Dobutamine (5)	962 ± 566*	5.80 ± 0.63	1.12 ± 0.67	26 ± 4	−1 ± 2	7 ± 15*	241 ± 167	−43 ± 112	89 ± 181
Oxfenicine (9)	373 ± 100	5.09 ± 0.86	1.46 ± 0.43	11 ± 12*	7 ± 5	51 ± 14	20 ± 23	216 ± 162	366 ± 173
Glucose (3)	89 ± 19	25.02 ± 5.15*	2.74 ± 0.76*	2 ± 4*	1 ± 1	43 ± 6	2 ± 2	166 ± 195	643 ± 217

*$p < 0.05$ compared with the control group.

Arterial concentration of long-chain fatty acids (FA), glucose and lactate (μmole/l for FA, mmole/l for glucose and lactate); myocardial utilization (nmole/g/min); and myocardial extraction fraction (%) [(arterial − coronary sinus) ÷ arterial concentration]. Values were obtained by direct sampling of arterial and coronary sinus blood. Utilization rates were obtained by calculating arterial-coronary sinus differences × MBF. Values represent the mean ± s.d.

estimation of oxidation of radiolabeled palmitate was determined by measuring myocardial $^{11}CO_2$ production multiplied by myocardial blood flow.

Statistical Analysis

All data are presented as the mean ± s.d. Correlations were calculated by linear regression. Differences between grouped data were compared using analysis of variance with the posthoc Scheffé test.

RESULTS

Metabolic Alterations

Twenty-three PET scans were obtained: six under control conditions, five during infusion of dobutamine, nine after administration of oxfenicine and three during glucose, insulin and potassium infusion. As summarized by the data in Table 1, heart rate and blood pressure increased slightly with low-dose dobutamine and were unchanged with oxfenicine. Heart rate

was slightly decreased in the 3 dogs receiving glucose. Myocardial oxygen consumption and blood flow followed these trends.

The data presented in Table 2 summarizes the wide range of metabolic conditions and rates of myocardial fatty acid utilization achieved. Total arterial long-chain fatty acid content averaged 367 μmole/l (range 237 to 618 μmole/l) under control conditions, increased significantly during dobutamine infusion, was without significant change after oxfenicine and decreased during glucose infusion. Steady-state total long-chain fatty acid extraction fraction decreased by more than 35% with dobutamine and was minimal after administration of oxfenicine or during glucose infusion. Although dobutamine infusion resulted in a decreased fatty acid extraction fraction, fatty acid utilization increased because arterial fatty acid concentration increased by nearly threefold and flow also increased. Glucose extraction and utilization were enhanced by administration of

TABLE 3
Summary of Individual Long-chain Fatty Acids, Arterial Concentration, Myocardial Extraction and Utilization

Group (n)	Arterial concentration			Extraction fraction (%)	Utilization rate (%)	
	Species	μmole/l	% total		nmole/g/min	% total
Control (6)	14:0	6 ± 2	1 ± 0.2	18 ± 91	1 ± 3	0.4 ± 3
	16:0	115 ± 28	27 ± 2	31 ± 6	27 ± 8	23 ± 3
	16:1	29 ± 10	7 ± 2	53 ± 22	11 ± 3	9 ± 2
	18:0	67 ± 26	16 ± 6	18 ± 5	9 ± 3	8 ± 3
	18:1	147 ± 54	33 ± 6	46 ± 8	53 ± 24	43 ± 6
	18:2	73 ± 19	17 ± 10	36 ± 8	20 ± 6	17 ± 2
Dobutamine (5)	14:0	14 ± 9	1 ± 0.3	16 ± 27	1 ± 5	−0.7 ± 3
	16:0	231 ± 122*	24 ± 4	22 ± 11	53 ± 33	11 ± 20
	16:1	85 ± 68	7 ± 2	24 ± 4	19 ± 18	0.2 ± 13
	18:0	111 ± 43	13 ± 5	8 ± 28	18 ± 19	8 ± 5
	18:1	461 ± 305	39 ± 7	31 ± 11	140 ± 111	48 ± 10
	18:2	176 ± 116	16 ± 2	21 ± 16	45 ± 33	19 ± 7
Oxfenicine (9)	14:0	5 ± 2	1 ± 0.2	12 ± 7	0.3 ± 0.2	0.8 ± 2
	16:0	115 ± 31	27 ± 2	9 ± 6*	5 ± 3*	25 ± 12
	16:1	30 ± 12	7 ± 1	10 ± 27*	2 ± 2	3 ± 24
	18:0	67 ± 24	16 ± 4	−6 ± 10	−0.9 ± 2	8 ± 38
	18:1	135 ± 47	31 ± 5	15 ± 7*	10 ± 7	41 ± 34
	18:2	77 ± 27	18 ± 2	9 ± 9*	3 ± 3	22 ± 15
Glucose (3)	14:0	2 ± 2	2 ± 2	67 ± 47	1 ± 1	36 ± 45
	16:0	31 ± 5	30 ± 1	12 ± 8*	2 ± 1	60 ± 50
	16:1	5 ± 3	4 ± 3	8 ± 31	0.5 ± 1	−3 ± 24
	18:0	29 ± 2	28 ± 5	−9 ± 8	−2 ± 1	−30 ± 6
	18:1	26 ± 8	24 ± 4	9 ± 14*	2 ± 3	26 ± 44
	18:2	14 ± 1	13 ± 1	5 ± 5*	0.4 ± 0.3	11 ± 14

*$p < 0.05$ compared with control.
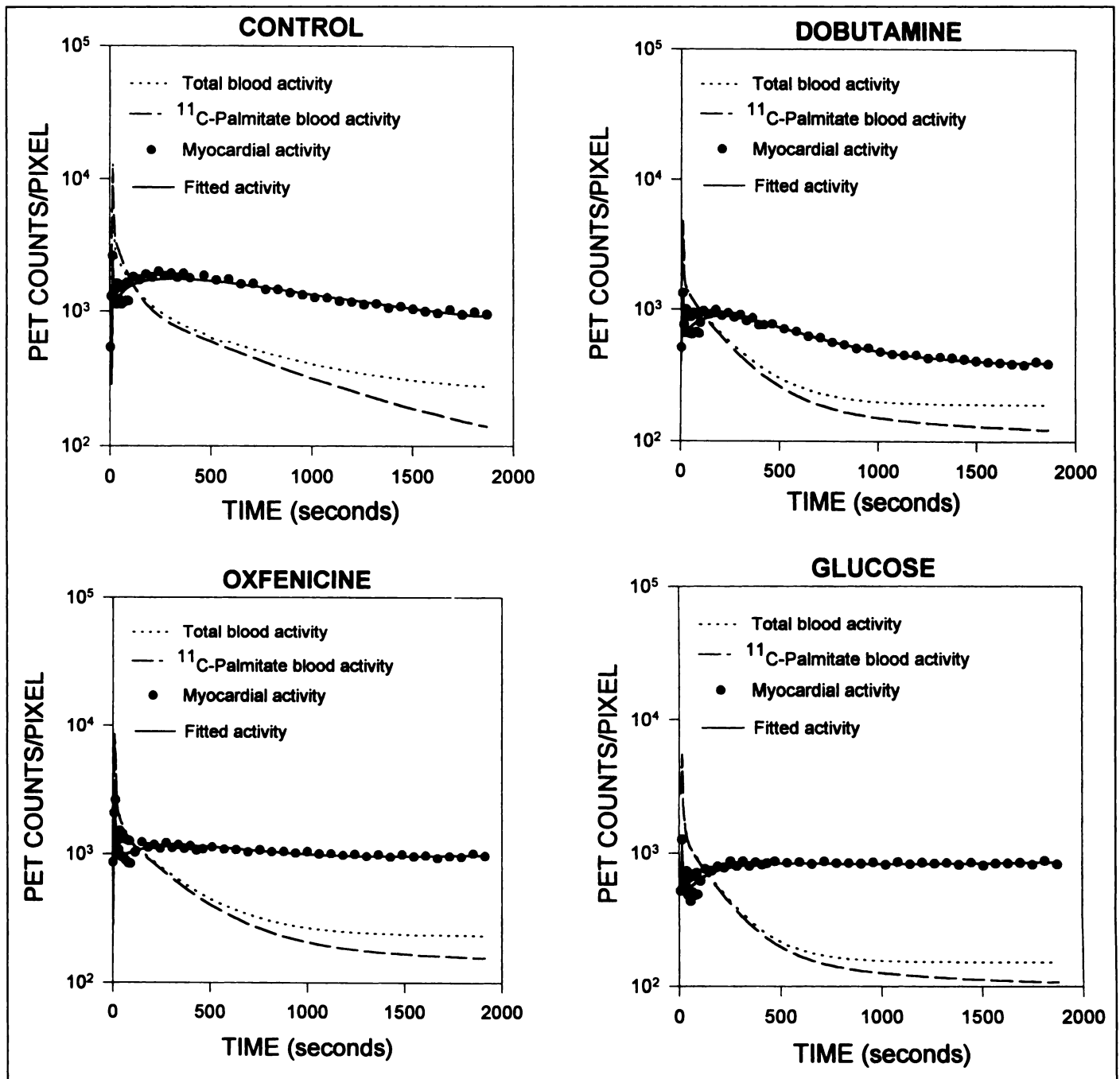Values represent the mean ± s.d.

FIGURE 2. Time-activity curves from representative dogs in the different groups. The mathematical model fitted curves extremely well under all conditions studied.

oxfenicine and glucose infusion, but the changes did not reach statistical significance because of the small arterial-coronary sinus differences and number of animals studied (Table 2). Although total arterial long-chain fatty acid content varied with the interventions, the proportion of individual fatty acids and their myocardial extraction remained relatively constant (Table 3).

Analysis of PET Data

Time-activity curves from representative dogs are presented in Figure 2. Clearance of labeled palmitate from blood was rapid (approximately 10% of peak by 10 min after administration of tracer) and did not vary markedly among the groups. In contrast, the shape of myocardial time-activity curves did vary, with the most rapid curves seen during dobutamine infusion, and flatter curves observed after oxfenicine and during glucose

infusion. The resultant model curves fitted observed data extremely well (Fig. 2).

Table 4 presents the results of turnover rate constant estimations. Value k_n reflects the rate of transport of label from one compartment to the other (Fig. 1). For example, increases in k_2 represent increased back-diffusion from the cytosol or interstitial space into the vascular space. Although the rates of transport from one compartment to the other are useful in their own right, as outlined in the Appendix, we modified the approach proposed by De Grado et al. (32) to use these rates of transport to define steady-state rates of myocardial palmitate utilization as well as to estimate the fraction of extracted 1-^{11}C-palmitate that was either oxidized or esterified to neutral lipids (or entered other slow turnover pools).

Figure 3 shows the close correlation between the modeled

TABLE 4
Summary of Turnover Rate Constants

Group (n)	k_1	k_2	k_3	k_4	k_5
Control (6)	6.22 ± 0.62	0.113 ± 0.032	0.016 ± 0.008	0.032 ± 0.066	0.082 ± 0.024
Dobutamine (5)	6.26 ± 0.47	0.073 ± 0.046	0.019 ± 0.004	0.005 ± 0.012	0.087 ± 0.017
Oxfenicine (9)	5.66 ± 0.62	0.150 ± 0.045	0.038 ± 0.018	0.001 ± 0.002	0.020 ± 0.014*
Glucose (3)	5.38 ± 0.83	0.162 ± 0.069	0.070 ± 0.087	0.017 ± 0.015	0.006 ± 0.006*

*p < 0.05 compared with the control group.

Summary of turnover rate constants (min^{-1}) obtained from the mathematical model (Fig. 1). k_1 represents the flux of tracer from the vasculature into the cell; k_2 represents back-diffusion; k_3 represents influx of tracer into the neutral lipid pool; k_4 represents the egress from the neutral lipid pool; and k_5 represents entry into mitochondrial oxidation. Values represent the mean ± s.d.

and directly measured rates of myocardial steady-state palmitate utilization. Figure 4 demonstrates that modeled steady-state palmitate utilization correlated with steady-state *total* myocardial fatty acid utilization as well since palmitate made up a relatively stable proportion of total arterial fatty acids as well as a relatively stable fraction of the fatty acid extracted and utilized by the myocardium (Table 3).

Under control circumstances or with dobutamine, > 80% of extracted palmitate underwent oxidation (Fig. 5). After oxfenicine or during glucose infusion, the fractions undergoing oxidation decreased, whereas the fractions that underwent esterification (or entered another slow turnover pool) greatly increased (p < 0.05 for each compared with controls). Model-estimated fractional oxidation correlated closely with directly measured palmitate oxidation (r = 0.87, p < 0.001).

DISCUSSION

Abnormalities in cellular metabolism presage contractile dysfunction as well as cardiac arrhythmias. PET offers a powerful approach to noninvasively estimate abnormalities in myocardial fatty acid metabolism and has already been used successfully in defining modalities that enhance salvage from myocardial ischemia (11,18–20); the metabolic patterns of substrate use which define viable from nonviable myocardium

(34,35); and identifying abnormalities that occur with both inherited and acquired cardiomyopathies (25,26).

The interventions chosen were employed to alter fatty acid utilization and oxidation over a wide range by varying intracellular pathways as well as arterial fatty acid content. Model estimated utilization correlated closely with directly measured utilization over the wide range induced (Figs. 3 and 4). The model-estimated amount of extracted palmitate undergoing oxidation under control conditions averaged 84%, a value which agreed extremely closely with direct measurements and with previous values from our laboratory (21,22). With dobutamine, arterial fatty acid increased markedly as anticipated based on the lipolytic effects of beta-adrenergic stimulation. Steady-state extraction fraction of fatty acid was diminished slightly. Oxfenicine, a relatively selective and potent inhibitor of carnitine palmitoyltransferase I (28–30), did not induce alterations in arterial fatty acid content or hemodynamics, but markedly impaired fatty acid oxidation and its administration was accompanied by enhanced myocardial glucose utilization. Esterification and deposition into neutral lipid pools as well as back-diffusion were enhanced, and these changes were detectable with the approach developed (Tables 3 and 4, Fig. 5). Glucose infusion was accompanied by a profound decrease in arterial fatty acid content and enhanced myocardial use of
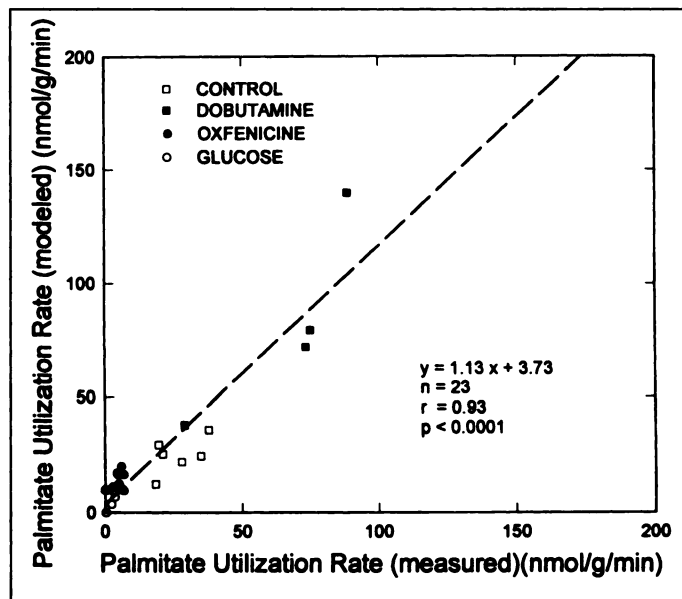

FIGURE 3. Correlation between modeled steady-state palmitate utilization and steady-state palmitate utilization evaluated by direct arterial-coronary sinus sampling. The correlation was excellent over the wide range of rates studied.
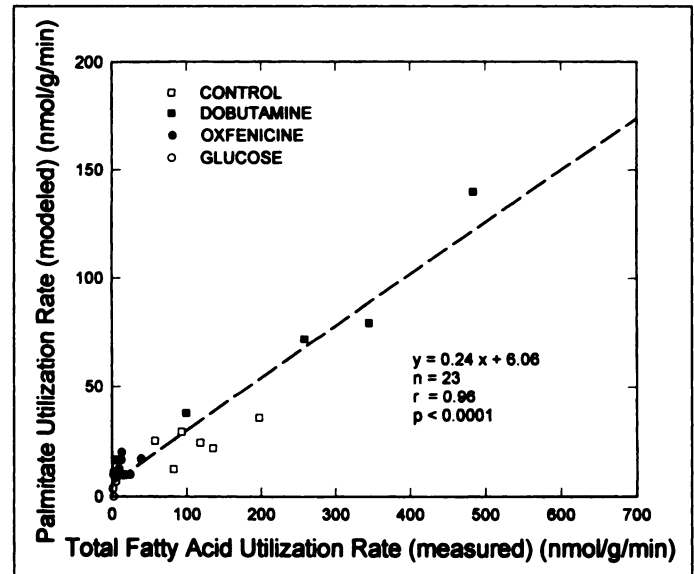

FIGURE 4. Correlation between modeled steady-state palmitate utilization and steady-state *total* long-chain fatty acid utilization measured directly. The correlation was excellent because the proportion of palmitate to total arterial fatty acid did not change (Table 3) and utilization of palmitate represented a stable fraction of total long-chain use.
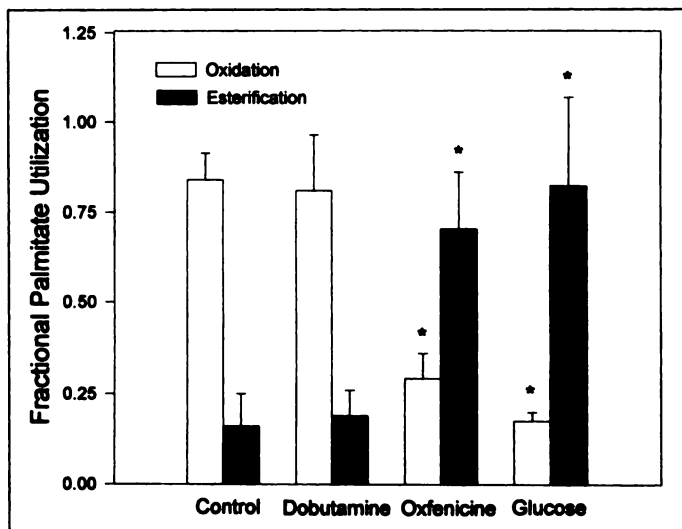
FIGURE 5. Histogram of the fraction of extracted palmitate undergoing oxidation or esterification (or entry into other slow turnover pools) as estimated with the model.

glucose. Extracted fatty acid during glucose infusion exhibited increased back-diffusion as well as increased shunting to storage forms (Table 4 and Fig. 5). The wide variation of flow, work and pattern of substrate use covers the range that might be encountered clinically in patients with inherited or acquired cardiomyopathy. Alterations that accompany myocardial ischemia may be more difficult to assess accurately because decreased perfusion would likely decrease signal-to-noise, although this has not been tested directly.

The mathematical model developed, although highly simplified from the known biochemical fate of fatty acid use by the heart, appears to adequately characterize observed myocardial time-activity curves (Fig. 2) and correlated extremely well with directly measured steady-state utilization (Figs. 3 and 4). In addition, the mathematical model permitted determination of the amount of extracted palmitate that underwent oxidation from that undergoing esterification (or incorporation to other slow turnover pools) suggesting that the magnitude as well as the loci of abnormal metabolism is detectable with the approach developed.

Recent data from our laboratory have demonstrated that with the approach described, differences in the handling of fatty acid by the myocardium can be distinguished in patients with inherited abnormalities of fatty acid metabolism compared to those with acquired cardiomyopathy (27,36).

Technical Considerations

Although more complex compartmental models could have been defined, we limited the approach to the four-compartment model schematized in Figure 1 because experience has demonstrated that the maximum number of parameters that can be accurately and reliably measured with PET is limited by the dynamic data available and the model configuration. Greater numbers of parameters can, of course, be estimated, but they become unreliable due to high correlations among parameters as well as high variance of the estimates.

Although the approach developed appears promising, a number of caveats are warranted. In the present study, the arterial input curve was corrected for conversion of palmitate to $^{11}CO_2$. As shown in Figure 2, this correction only modestly affected the shape of the input curve. If the input curve is not corrected for $^{11}CO_2$, k_3 (the rate of transfer to triglycerides) and the fractional esterification rate are the only estimates that are significantly

affected (decreased, data not shown), as would be anticipated since they are represented by the tail of the time-activity curve. A normalized correction for conversion of arterial palmitate to $^{11}CO_2$ may be acceptable if validated in humans. Although arterial substrate content was used in the present study, venous fatty acid levels would likely be measured during clinical studies. The difference between arterial and venous fatty acid content under steady-state conditions is modest (and was less than 10% in paired measurements in our laboratory).

With regard to the mathematical model, V, the vascular volume was fixed at 0.1 ml/g tissue in the present study. Although this seems reasonable based on the known vascular volume of myocardium, some disease states, especially myocardial ischemia and reperfusion may alter the vascular volume. Sensitivity analysis will be needed to define the magnitude of error that would be induced under these circumstances.

It should be recognized that the label used in this study was 1-^{11}C-palmitate. Although palmitate cannot be used to define the utilization of all long-chain fatty acids within the myocardium since each is extracted and utilized to a different extent based on its chain length as well as its arterial concentration, palmitate does normally account for approximately 25% of all fatty acids used by the myocardium, represents approximately 25%–30% of arterial fatty acids (Table 3) and is the prototype for long-chain fatty acids. Since the percentage of palmitate to total fatty acids did not change during the interventions (Table 3), and since the steady-state extraction fraction of each long-chain fatty acid remained relatively constant, modeled palmitate oxidation correlated quite closely with steady-state total long-chain myocardial fatty acid utilization (Fig. 4), although this relationship might be altered in some pathological conditions. Specific metabolism of other long-chain fatty acids of interest could be approached in a similar fashion.

Finally, although myocardial oxidation of 1-^{11}C-palmitate to $^{11}CO_2$ was measured directly and was well estimated with the model, esterification was not measured directly in the present study and fractional esterification could reflect shunting of label to other metabolic pathways. Nonetheless, under control conditions, rates of esterification estimated with the model agree with rates previously measured by our lab (21,22).

CONCLUSION

Myocardial palmitate metabolism can be defined with PET using 1-^{11}C-palmitate. The approach should enable enhanced understanding of the pathophysiology of the biochemical defects that underlie cardiac dysfunction and should also provide an objective means to test therapeutic strategies. We have previously shown that alteration of fatty acid delivery to hearts isolated from diabetic rabbits is associated with contractile improvement (37). The approach developed should aid in defining whether the changes in fatty acid metabolism presage or simply correlate with contractile dysfunction, predict recovery of function and whether altered metabolism, induced either pharmacologically or ultimately with gene therapy, will result in improved fatty acid handling and contractile function.

APPENDIX

The kinetics of fatty acids were described in the present study by a four-compartment model (Fig. 1) which defines tracer in the vascular space, in the interstitial space and cytosol, in neutral lipids, amino acids (or other slow-turnover pools) and in mitochondria. k_n represents the rate constant describing the transfer of tracer from one compartment to another. The model assumes that tracer entering the mitochondria is unidirectional and that metabolites are

washed out of the mitochondria into the vasculature at a rate proportional to flow.

The differential equations describing the model are:

$$\frac{\partial q_1}{\partial t} = F\left[Ca(t) - \frac{q_1}{V}\right] + k_2 \qquad \text{Eq. A1}$$

$$\frac{\partial q_2}{\partial t} = k_1 q_1 + k_4 q_3 - (k_2 + k_3 + k_5)q_2 \qquad \text{Eq. A2}$$

$$\frac{\partial q_3}{\partial t} = k_3 q_2 - k_4 q_3 \qquad \text{Eq. A3}$$

$$\frac{\partial q_4}{\partial t} = k_5 q_2 - \frac{F}{V} q_4 \qquad \text{Eq. A4}$$

and total tracer concentration in myocardium at any given time can be defined by the sum of the tracer in each compartment:

$$q_T(t) = q_1(t) + q_2(t) + q_3(t) + q_4(t) \qquad \text{Eq. A5}$$

where:

F = flow (ml/g/min)

Ca(t) = arterial tracer concentration (CPM/ml)

k_1, k_2 = rate constants describing the transfer of ^{11}C from the vasculature to the intracellular compartment and the reverse process (min^{-1})

k_3, k_4 = rate constants describing the incorporation of ^{11}C into amino acids, neutral lipids or other slow turnover processes and the reverse process, respectively (min^{-1})

k_5 = rate constant describing the transport of ^{11}C into the mitochondria (min^{-1}) (assumed to be unidirectional)

V = fractional vascular volume (assumed to be 10% of total volume) (ml/g)

q_n = concentration of tracer in compartment n (CPM/ml)

q_T = the total concentration of tracer in myocardium (CPM/ml).

To estimate the rate constants from the compartmental model, the arterial tracer concentration [(the input function, Ca(t)] must be known. The arterial blood activity obtained from PET images represents not only ^{11}C-palmitate but also $^{11}CO_2$ produced from β-oxidation. To define the true input function, arterial blood activity must be corrected for $^{11}CO_2$. The fraction of ^{11}C-palmitate in blood as a function of time was obtained by subtracting the contribution of $^{11}CO_2$, obtained by direct sampling of blood, from total ^{11}C-activity in arterial blood. A multiexponential function was fitted to this fraction so it could be defined at any point in time and used to correct the total ^{11}C-blood activity obtained from PET images. Flow was fixed to values obtained with microspheres and the fractional vascular volume (V) was fixed to 0.1 ml/g.

Since the numerical method used to solve the partial differential equations of the compartmental model requires the evaluation of the input function at any point in time, the input function had to be defined analytically. This was accomplished by fitting the input function to a gamma variate function splined with a multiexponential function.

Myocardial tracer concentration cannot be measured directly with PET due to partial volume and spillover effects. Partial volume, the underestimation of true tracer concentration, and count spillover, the contamination of activity in one region due to radioactivity from an adjacent one, are observed when imaging an object small with respect to the resolution of the tomograph. PET tissue activity $q_{T_{PET}}(t)$, can be related to the true tissue activity, $q_T(t)$, and the blood activity, $q_B(t)$, partial volume and spillover effects by the equation:

$$q_{T_{PET}}(t) = F_{MM}q_T(t) + F_{BM}q_B(t) \qquad \text{Eq. A6}$$

where:

$q_{T_{PET}}(t)$ = PET tissue tracer concentration (CPM/ml)

$q_B(t)$ = true arterial blood tracer concentration (CPM/ml) and

F_{MM} = tissue recovery coefficient

F_{BM} = spillover fraction of blood activity observed in tissue, and

$q_T(t)$ is defined as in Equation A5. By replacing $q_T(t)$ in Equation A6 by Equation A5 a new operational equation is obtained where the parameters to be estimated are the model rate constants plus the two PET parameters F_{MM} and F_{BM}.

The system of differential equations describing the mass transfer of the tracer compartmental models was solved numerically using the IMSL library routine IVPAG and Gear's backward differentiation formulas. The IMSL routine BCLSF, used to estimate the seven parameters, solves the nonlinear, least squares problem using a modified Levenberg-Marquardt algorithm and a finite-difference Jacobian.

Steady-state palmitate back-diffusion (BD), esterification (ES) and oxidation (OX) in nmole/g/min were derived from the kinetic model:

$$BD = k_2 q_2 \qquad \text{Eq. A7}$$

$$ES = k_3 q_2 \qquad \text{Eq. A8}$$

$$OX = k_5 q_2 \qquad \text{Eq. A9}$$

where Equation A8 assumes that k_4 is negligible, and q_2 is the concentration of unlabeled palmitate in compartment 2.

From steady-state conditions:

$$q_2 = \frac{k_1}{k_2 + k_5} q_1 \qquad \text{Eq. A10}$$

where q_1 is the concentration of unlabeled palmitate in compartment 1 (arterial blood).

Since at steady-state there is no change in the net amount of palmitate in each compartment, q_1 can be obtained by setting Equation A1 to zero:

$$\frac{\partial q_1}{\partial t} = FCa - \frac{F}{V} q_1 + k_2 q_2 - k_1 q_1 = 0 \qquad \text{Eq. A11}$$

where:

F = flow (ml/g/min)

$V = V_1 = 0.1$ ml/g

Ca = palmitate concentration in arterial blood (μmole/liter).

Substituting Equation A10 into Equation A11 we obtain:

$$FCa - \frac{F}{V} q_1 + \left(\frac{k_1 k_2}{k_2 + k_5}\right)q_1 - k_1 q_1 = 0. \quad \text{Eq. A12}$$

Collecting terms:

$$\text{and:} \quad FCa = \left[\left(\frac{F}{V} + k_1\right) - \left(\frac{k_1 k_2}{k_2 + k_5}\right)\right]q_1 \qquad \text{Eq. A13}$$

$$q_1 = \frac{FCa}{\left(\dfrac{F}{V} + k_1\right) - \dfrac{k_1 k_2}{k_2 + k_5}}$$

$$= \frac{(k_2 + k_5)}{(k_2 + k_5)\left(\dfrac{F}{V} + k_1\right) - k_1 k_2} FCa. \qquad \text{Eq. A14}$$

Substituting Equation A14 into Equation A10:

$$q_2 = k_1 \left[\frac{FCa}{(k_2 + k_5)\left(\dfrac{F}{V} + k_1\right) - k_1k_2} \right]. \quad \text{Eq. A15}$$

Substituting Equation A15 into Equations A7–9:

$$BD = k_1k_2 \left[\frac{FCa}{(k_2 + k_5)\left(\dfrac{F}{V} + k_1\right) - k_1k_2} \right] \quad \text{Eq. A16}$$

$$ES = k_1k_3 \left[\frac{FCa}{(k_2 + k_5)\left(\dfrac{F}{V} + k_1\right) - k_1k_2} \right] \quad \text{Eq. A17}$$

$$OX = k_1k_5 \left[\frac{FCa}{(k_2 + k_5)\left(\dfrac{F}{V} + k_1\right) - k_1k_2} \right]. \quad \text{Eq. A18}$$

Total utilization (U) in nmole/g/min is defined as:

$$U = ES + OX. \quad \text{Eq. A19}$$

The fraction of extracted palmitate which undergoes esterification (F_{ES}) or oxidation (F_{OX}) were computed from Equations A17 and A18 as:

$$F_{ES} = \frac{ES}{ES + OX} \quad \text{Eq. A20}$$

$$F_{OX} = \frac{OX}{ES + OX}. \quad \text{Eq. A21}$$

ACKNOWLEDGMENTS

REFERENCES

1. Bing RJ. Cardiac metabolism. *Physiol Rev* 1965;45:171–213.
2. Lietdke AJ. Alterations of carbohydrate and lipid metabolism in the acutely ischemic heart. *Prog Cardiovasc Dis* 1981;23:321–336.
3. Neely JR, Morgan HE. Relationship between carbohydrate and lipid metabolism and the energy balance of heart muscle. *Ann Rev Physiol* 1974;36:413–459.
4. Camici P, Ferrannini E, Opie LH. Myocardial metabolism in ischemic heart disease: basic principles and application to imaging by positron emission tomography. *Prog Cardiovasc Dis* 1989;32:217–238.
5. Hale DE, Bennett MJ. Fatty acid oxidation disorders: a new class of metabolic diseases. *J Pediatr* 1992;121:1–11.
6. Paulson DJ, Noonan JJ, Ward KM, et al. Effects of POCA on metabolism and function in the ischemic rat heart. *Basic Res Cardiol* 1986;81:180–187.
7. Corr PB, Creer MH, Yamada KA, et al. Prophylaxis of early ventricular fibrillation by inhibition of acylcarnitine accumulation. *J Clin Invest* 1989;83:927–936.
8. Myears DW, Sobel BE, Bergmann SR. Substrate use in ischemic and reperfused canine myocardium: quantitative considerations. *Am J Physiol:Heart Circ Physiol* 1987;253: H107–H114.
9. Trauner DA, Horvath E, Davis LE. Inhibition of fatty acid beta-oxidation by influenza B virus and salicylic acid in mice: implications for Reye's syndrome. *Neurology* 1988;38:239–241.
10. Deschamps D, Fisch C, Fromenty B, et al. Inhibition by salicylic acid of the activation and thus oxidation of long-chain fatty acids. Possible role in the development of Reye's syndrome. *J Pharmacol Exp Ther* 1991;259:894–904.
11. Lerch RA, Bergmann SR, Sobel BE. Delineation of myocardial fatty acid metabolism with positron emission tomography. In: Bergmann SR, Sobel BE, eds. *Positron emission tomography of the heart*. Mount Kisco, NY: Futura Publishing, Inc.; 1992: 129–152.
12. Goldstein RA, Klein MS, Welch MJ, Sobel BE. External assessment of myocardial metabolism with Carbon-11-palmitate in vivo. *J Nucl Med* 1980;21:342–348.
13. Schön HR, Schelbert HR, Robison G, et al. Carbon-11-labeled palmitic acid for the noninvasive evaluation of regional myocardial fatty acid metabolism with positron-computed tomography. I. Kinetics of Carbon-11-palmitic acid in normal myocardium. *Am Heart J* 1982;103:532–547.
14. Schön HR, Schelbert HR, Najafi A, et al. Carbon-11-labeled palmitic acid for the noninvasive evaluation of regional myocardial fatty acid metabolism with positron-computed tomography. II. Kinetics of Carbon-11-palmitic acid in acutely ischemic myocardium. *Am Heart J* 1982;103:548–561.
15. Schelbert HR, Henze E, Keen R, et al. Carbon-11-palmitate for the noninvasive evaluation of regional myocardial fatty acid metabolism with positron-computed tomography. IV. In vivo evaluation of acute demand-induced ischemia in dogs. *Am Heart J* 1983;106:736–750.
16. Ter-Pogossian MM, Klein MS, Markham J, Roberts R, Sobel BE. Regional assessment of myocardial metabolic integrity in vivo by positron-emission tomography with ^{11}C-labeled palmitate. *Circulation* 1980;61:242–255.
17. Sobel BE, Weiss, Welch MJ, et al. Detection of remote myocardial infarction in patients with positron emission transaxial tomography and intravenous. ^{11}C-palmitate *Circulation* 1977;55:853–857.
18. Bergmann SR, Fox KAA, Ter-Pogossian MM, et al. Clot-selective coronary thrombolysis with tissue-type plasminogen activator. *Science* 1983;220:1181–1183.
19. Knabb RM, Rosamond TL, Fox KAA, et al. Enhancement of salvage of reperfused ischemic myocardium by diltiazem. *J Am Coll Cardiol* 1986;8:861–871.
20. Sobel BE, Geltman EM, Tiefenbrunn AJ, et al. Improvement of regional myocardial metabolism after coronary thrombolysis induced with tissue-type plasminogen activator or streptokinase. *Circulation* 1984;69:983–990.
21. Fox KAA, Abendschein D, Ambos HD, et al. Efflux of metabolized and nonmetabolized fatty acid from canine myocardium. Implications for quantifying myocardial metabolism tomographically. *Circ Res* 1985;57:232–243.
22. Rosamond TL, Abendschein DR, Sobel BE, et al. Metabolic fate of radiolabeled palmitate in ischemic canine myocardium: implications for positron-emission tomography. *J Nucl Med* 1987;28:1322–1329.
23. Schelbert HR, Henze E, Schön HR, et al. Carbon-11-palmitate for the noninvasive evaluation of regional myocardial fatty acid metabolism with positron-computed tomography. III. In vivo demonstration of the effects of substrate availability on myocardial metabolism. *Am Heart J* 1983;105:492–504.
24. Schelbert HR, Henze E, Sochor H, et al. Effects of substrate availability on myocardial Carbon-11-palmitate kinetics by positron-emission tomography in normal subjects and patients with ventricular dysfunction. *Am Heart J* 1986;111:1055–1064.
25. Kelly DP, Mendelsohn NJ, Sobel BE, Bergmann SR. Detection of impaired myocardial fatty acid utilization by positron-emission tomography indicative of genetic deficiency of long-chain acyl-CoA dehydrogenase. *Am J Cardiol* 1993;71:738–744.
26. Sochor H, Schelbert HR, Schwaiger M, et al. Studies of fatty acid metabolism with positron-emission tomography in patients with cardiomyopathy. *Eur J Nucl Med* 1986;12:S66–S69.
27. Bergmann SR, Rubin, PR, Hartman JJ, Herrero P. Detection of abnormalities in fatty acid metabolism in patients with cardiomyopathy using PET [Abstract]. *J Nucl Med* 1995;36:142P.
28. Higgins AJ, Morville M, Burges RA, Blackburn KJ. Mechanism of action of oxfenicine on muscle metabolism. *Biochem Biophys Res Comm* 1981;100:291–296.
29. Bachmann E, Weber E. Biochemical mechanisms of oxfenicine cardiotoxicity. *Pharmacology* 1988;36:238–248.
30. Bielefeld DR, Vary TC, Neely JR. Inhibition of carnitine palmitoyl-CoA transferase activity and fatty acid oxidation by lactate and oxfenicine in cardiac muscle. *J Mol Cell Cardiol* 1985;17:619–625.
31. Welch MJ, Dence CS, Marshall DR, Kilbourn MR. Remote system for production of carbon-11-labeled palmitic acid. *J Labeled Compds Radiopharm* 1983;20:1087–1095.
32. DeGrado TR, Holden JE, Ng CK, et al. Quantitative analysis of myocardial kinetics of 15-p-[iodine-125] iodophenylpentadecanoic acid. *J Nucl Med* 1989;30:1211–1218.
33. Bergmann SR, Carlson E, Dannen E, Sobel BE. An improved assay with 4-(2-thiazolylazo)-resorcinol for free fatty acids in biological fluids. *Clin Chim Acta* 1980;104:53–63.
34. Lerch RA, Ambos HD, Bergmann SR, et al. Localization of viable but ischemic myocardium by positron emission tomography (PET) with. ^{11}C-palmitate. *Circulation* 1981;64:689–699.
35. Grover-McKay M, Schelbert HR, Schwaiger M, et al. Identification of impaired metabolic reserve by atrial pacing in patients with significant coronary artery stenosis. *Circulation* 1986;74:281–292.
36. Bergmann SR, Herrero P, Hartman JJ, et al. Quantitative assessment of myocardial fatty acid metabolism in pediatric patients with inherited cardiomyopathy [Abstract]. *Circulation* 1995;92:I-444.
37. Fields LE, Daugherty A, Bergmann SR. Effect of fatty acid on performance and lipid content of hearts from diabetic rabbits. *Am J Physiol:Heart Circ Physiol* 1986;250: H1079–H1085.